PHYSICAL REVIEW B **93**, 201404(R) (2016)

Superlubricity in quasicrystalline twisted bilayer graphene

Elad Koren* and Urs Duerig
IBM Research–Zurich, 8803 Rueschlikon, Switzerland
(Received 11 April 2016; published 31 May 2016)

The unique atomic positions in quasicrystals lead to peculiar self-similarity and fractal-like structural morphology. Accordingly, many of the material properties are supposed to manifest exceptional characteristics. In this Rapid Communication, we explain through numerical simulations the fundamental and peculiar aspects of quasicrystals wearless friction manifested in a 30° twisted bilayer graphene system. In particular, the sliding force exhibits a fractal structure with distinct area correlations due to the natural mixture between both periodic and aperiodic lateral modulations. In addition, zero power scaling of the sliding force with respect to the contact area is demonstrated for a geometric sequence of dodecagonal elements.

DOI: 10.1103/PhysRevB.93.201404

The discovery of quasicrystals [1,2] (QCs) has dramatically redefined the basic definition of crystals in the crystallography community. A QC is a crystalline structure that breaks the periodicity of a normal crystal for an ordered, yet aperiodic, arrangement, lacking any translational symmetry. Consequently, the diffraction pattern of QCs is characterized by sharp and discrete peaks which follow rotational symmetries forbidden to ordinary crystals.

Closely related interfaces exhibiting quasicrystal symmetry have attracted much attention as a class of interesting tribological materials manifesting anomalously low friction coefficients [3–5]. However, up to now, the physical origin of the low friction properties is considered to be an open question. In particular, it is not clear to what extent the peculiar aperiodic structure influences the sliding force and energy dissipation of such interfaces [5–7].

In general, the low friction phenomenon in incommensurate sliding surface contacts, termed structural superlubricity [8–10], is explained by a virtually zero energy barrier due the lack of crystal symmetry. Similarly, it can be interpreted in terms of an efficient cancellation of the sliding forces experienced by different parts of the moving contact [11–13]. It is a long-standing question in tribology whether true superlubricity, characterized by zero power scaling of the sliding force F with respect to the contact area A, i.e., $F \propto A^{\gamma}$, where $\gamma = 0$, really exists. The latter is suggested by theory for the case of infinitely large incommensurate contacts [11,12] and is yet to be experimentally demonstrated [13–16]. It is commonly accepted that for the two-dimensional (2D) case nonzero power scaling is inevitable due to symmetry breaking effects at the contact edges [17], whereas in the one-dimensional (1D) case, e.g., in double wall carbon nanotube structures, a constant sliding force independent of the tube length has been predicted [18].

In this Rapid Communication, we study a bilayer graphene interface with a rotational misfit of 30° which forms a dodecagonal QC interface structure [19]. We reveal through numerical simulations the fundamental and peculiar aspects of QC wearless friction. We demonstrate that the sliding force exhibits a fractal structure with distinct area correlations. In addition, zero scaling of the sliding force is demonstrated for a geometric sequence of dodecagonal elements, intricately connected to the fine and perfect force cancellation emerging from the quasiperiodic symmetry of the interface.

The atomic positions of a 30° twisted bilayer graphene interface follow a perfect quasiperiodic dodecagonal pattern (Fig. 1). A dodecagonal lattice holds 12-fold rotational symmetry due to a distinct distance that characterizes the system in all 12 directions. The structure is obtained by covering the area with triangles and squares as structural elements [Fig. 1(b)] [20]. Since squares and triangles enclose angles of 90° and 60°, respectively, their combination leads to a distribution of edges along 12 directions with 30° intervals. The adjacent dodecagons consist of six triangles in the center which are surrounded by an alternating arrangement of six squares and triangles. The corresponding quasiperiodic lattice follows a strict rule that leads to a distinct self-similarity. The center of each dodecagon represents the corner of a similar larger dodecagonal structure with a radius scaled by an irrational factor of $2+\sqrt{3}$ [Figs. 1(b) and 1(c)]. The elementary scale unit is $a = L\cos(15^{\circ})$, where L denotes the moiré superlattice unit cell $L = a_{\dagger}/\sqrt{2-2\cos(\theta)}$ corresponding to a twist angle $\theta = 30^{\circ}$, where $a_{\dagger} = 2.46$ Å denotes the graphene lattice constant. In this Rapid Communication, a corresponds to the radius of the smallest dodecagonal structure (and not to the dodecagonal face as in other papers). The area in between adjacent dodecagons is also filled by squares (fourfold symmetry) and triangles (threefold symmetry) that are randomly pointing along one of the 12 quasiperiodic directions.

The 2D energy map for the same system is presented in Fig. 2(a). The energy map reflects the atomic interactions between the top and bottom layers. Simulations are based on the force field analytical model developed by Kolmogorov and Crespi [21]. The system is assumed to be fully rigid, which is a reasonable approximation considering the large in-plane stiffness of graphene and the rapidly varying in-plane potential modulations due to the short moiré superlattice period. The energy map holds exactly the same dodecagonal QC symmetry and the pseudodiffraction pattern calculated from the energy map [Fig. 2(b)] displays the hallmark 12-fold rotational symmetry. For comparison, both the energy map and pseudodiffraction pattern for Bernal stacked bilayer graphene showing sixfold rotational symmetry are presented in Figs. 2(c) and 2(d), respectively.

The sliding force is analyzed to study the friction characteristics of such QC structures. The connection with friction arises from the fact that energy dissipation is governed by

*Corresponding author: elk@zurich.ibm.com

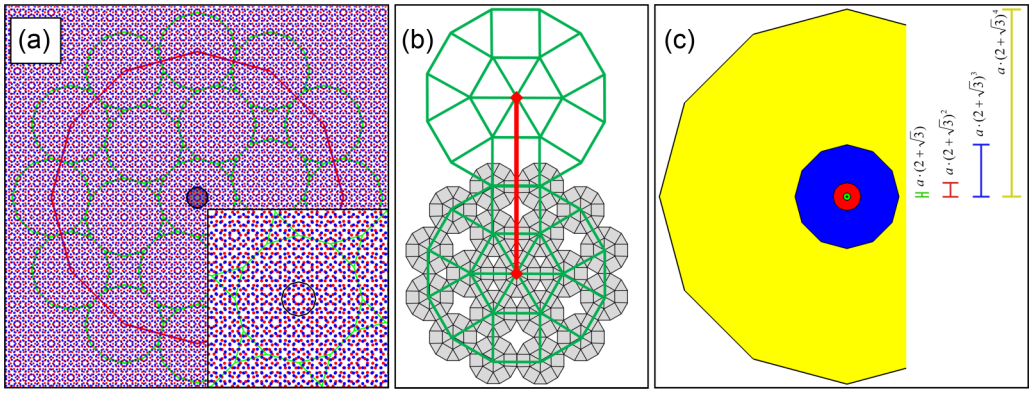

FIG. 1. (a) Atomic positions for 30° twisted bilayer graphene. Red and blue points correspond to the bottom and top graphene layers, respectively. The bilayer reveals a perfect quasiperiodic dodecagonal pattern. Black, green, and red colors represent dodecagonal structures with radii of a, $a(2+\sqrt{3})$, and $a(2+\sqrt{3})^2$, respectively. A magnified image of the central region is shown in the inset. (b) Each dodecagon consists of six triangles in the center which are surrounded by an alternating arrangement of six squares and triangles. The center of each dodecagon represents the corner of a similar larger dodecagonal structure with a radius scaled by an irrational factor $2+\sqrt{3}$. (c) Schematic representation of dodecagonal structures with radii $a(2+\sqrt{3})^n$ for $n = 1,2,3,4$.

spontaneous jumps from a marginally stable position to the next stable equilibrium position whenever the stiffness of the actuator is smaller than the negative value of the displacement force gradient along the slide direction. Therefore, the friction force basically scales with the magnitude of the sliding force fluctuations. To simulate sliding, the top flake is moved by a fixed increment of 0.01 nm along the high symmetry [1 1] axis pointing along an armchair orientation. At each position, a new energy map is calculated from which the force acting on the atoms in the flake, termed the force map, is derived by taking the numerical derivative along the slide axis. The overall sliding force experienced by different parts of the flake is then obtained by taking the sum over all atomic forces within the specific part.

In a first step, we calculate the sliding force signals of each of the 19 adjacent dodecagonal structures with a radius of $r = a(2+\sqrt{3})$, depicted in Fig. 2(a) in green. The dodecagonal structures containing 337 atoms each are fixed to the moving frame of the top sliding graphene layer. The sliding force signals are virtually identical in all of the structures. The force oscillations are very small in comparison to a Bernal stacked bilayer system of the same area and are within the same order of magnitude of a single sliding atom, i.e., ∼10 pN [13]. The same phenomenon is observed for all the other dodecagonal structures with $r = a(2+\sqrt{3})^n$ and $n = 0,2,3$ depicted in Fig. 1. Therefore, the sliding force of dodecagonal tiles of order n is perfectly correlated and the respective sliding forces add up coherently, as shown in Fig. 3(b).

A perfect correlation would lead to a simple scaling law of the sliding force with respect to the contact area $F \propto A$, if the structural voids between the adjacent dodecagons are neglected. This is rather a counterintuitive result considering that incommensurate sliding systems are typically characterized by a fractional scaling $F \propto A^{\gamma}$, where γ is predicted to be within the range of 0–0.5 depending on several properties of the contact such as geometry, crystallinity, orientation, and rim effects [12,16,17]. Next, we compare the sliding force signals of individual dodecagonal tiles with radii $r = a(2+\sqrt{3})^n$ and $n = 1,2,3,4$, i.e., $r = 17.13, 63.93, 238.61$, and 890.51 Å,

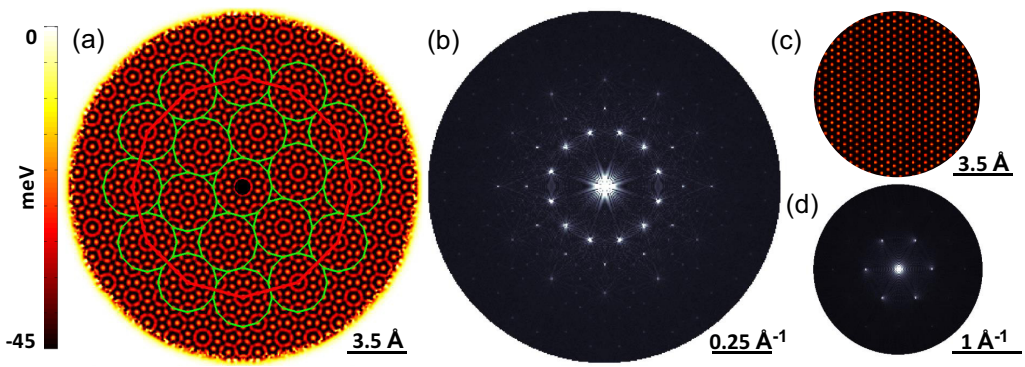

FIG. 2. (a) Energy map for 30° twisted bilayer graphene. The local atomic interactions between the top and bottom graphene layers reveal a perfect quasiperiodic dodecagonal pattern. Black, green, and red colors represent dodecagonal structures with radii of a, $a(2+\sqrt{3})$, and $a(2+\sqrt{3})^2$, respectively. (b) 2D pseudodiffraction pattern computed from the energy map. The 12-fold diffraction pattern is the signature of a QC layer with dodecagonal symmetry. For comparison, both the energy map (c) and pseudodiffraction pattern (d) for a Bernal stacked bilayer graphene system consisting of sixfold rotational symmetry are also presented. We note that due to the lower intensity of the higher-order peaks, only the first six reflexes are visible in (d).

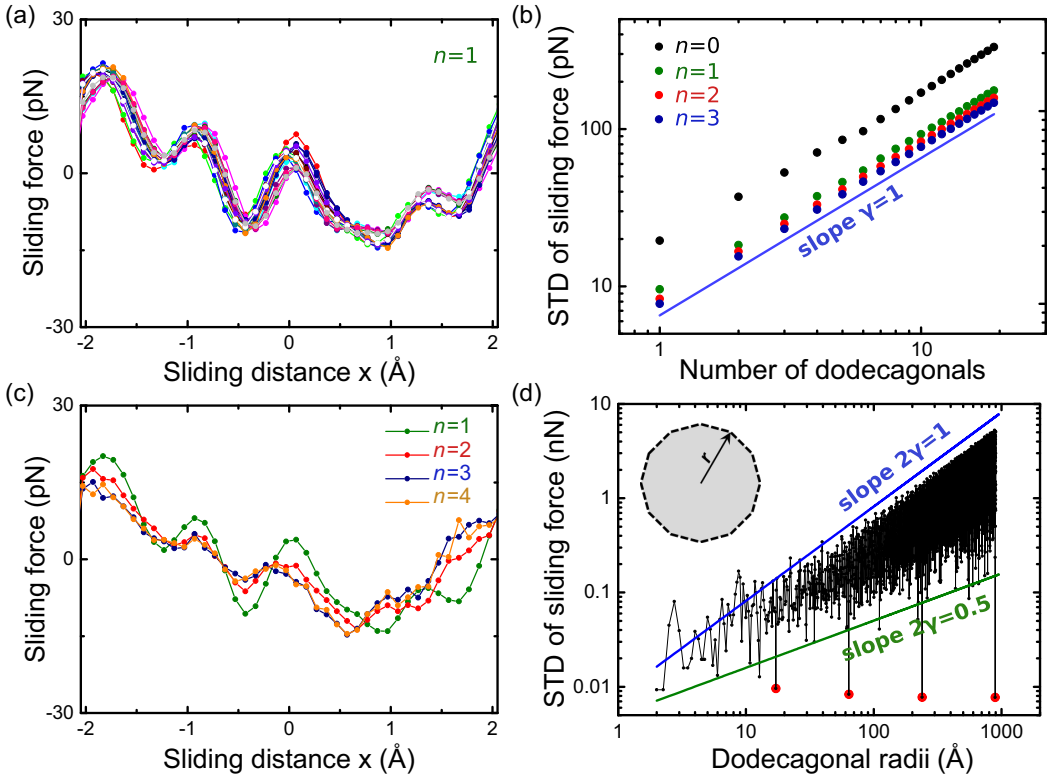

FIG. 3. (a) Sliding force profiles for the 19 adjacent dodecagonal structures shown in Fig. 1(a) in green. The structures have the same radial distance of $r = a(2 + \sqrt{3})$ and exhibit the same force profiles for sliding along the x direction. (b) The sliding force of dodecagonal tiles of order n is perfectly correlated and the respective sliding forces add up coherently (STD denotes the standard deviation of the sliding signal). (c) Sliding force profiles for four dodecagonal structures with radii of 17.13, 63.93, 238.61, and 890.51 Å, corresponding to $r = a(2 + \sqrt{3})^n$ with n being an integer between 1 and 4, produce virtually identical sliding force profiles. (d) Standard deviation of the sliding force signal for dodecagonal structures of different radii. The plot reveals three different scaling laws. For dodecagonal structures of $r = a(2 + \sqrt{3})^n$ and n being the integer, the force scales as $F \propto A^0$ (red dots). For noninteger values of n, two different scaling laws appear. In particular, the force oscillates between two power laws of $F \propto A^\gamma$, where γ is between 0.25 and 0.5, thus forming a growing "band" of possible force intensities. Inset: Geometrical definition of r for the dodecagonal structures.

comprising 337, 4680, 65 184, and 907 896 atoms, respectively [Fig. 3(c)]. Interestingly, the structures experience almost identical weak force signals, similar to the smallest dodecagon. For these fundamental tiling structures, the sliding force does not depend on the contact area and scales as $F \propto A^0$ [red spots in Fig. 3(d)].

For dodecagonal structures with a noninteger exponent in the radial equation, the sliding force scales with the contact area with an exponent $\gamma > 0$. Note that in this case the average number of atoms within different tiles will be an irrational noninteger number. Specifically, we observe large force variations constrained by two different power laws with $\gamma = 0.25$ and $\gamma = 0.5$ [Fig. 3(d)].

The two different observed scaling exponents can be explained by the structural correlation behavior of the dodecagonal QC. The larger scaling exponent of 0.5 is attributed to correlated rim forces which take place when consecutively adding new rows of atoms at the rim, e.g., the green dodecagonal parts which exceed beyond the red dodecagonal structure in Fig. 1(a). The smaller scaling exponent of 0.25 is likewise attributed to uncorrelated rim forces associated with the quasiperiodic nature of QC. Therefore, the overall force oscillates between correlated and uncorrelated rim contributions. The latter scaling

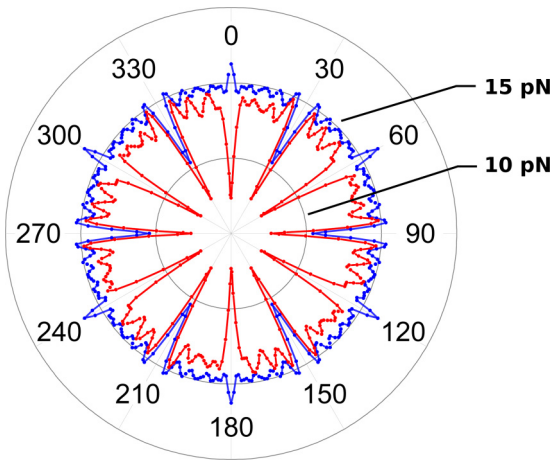

FIG. 4. Angular dependence of the force signal corresponding to a dodecagonal structure of $r = a(2 + \sqrt{3})^3$ (red) and for a single carbon atom (blue). The structures are moving along a straight, 5 Å long, line in different angular directions with respect to the high symmetry zigzag ([1 0]) orientation. In agreement with the crystal's lattice symmetries, the dodecagonal and the single carbon atom are characterized by 12-fold and sixfold rotational symmetry, respectively.

characteristics are typical for standard incommensurate (nonperiodic) systems [22] whereas the zero power scaling is a special property of QCs attributed to the fractal structural morphology.

The quasicrystal nature of the interface is also reflected in the angular dependence of the sliding force which exhibits 12-fold rotational symmetry. An example of an azimuthal plot for a dodecagonal structure with $n = 3$ is shown in Fig. 4. The force magnitude is similar to the one produced by a single sliding atom whereas the single atom force signal is showing sixfold rotational symmetry, in agreement with graphene lattice symmetry.

In conclusion, the quasiperiodic interlayer structure of a 30° twisted bilayer graphene system gives rise to nontrivial correlations between the sliding force and the contact geometry. We demonstrate that perfect superlubricity characterized by a scale invariant sliding force is obtained for the geometric sequence of fundamental dodecagonal tiling elements in the quasicrystal structure.

We thank Michael Urbakh for stimulating discussions. E.K. gratefully acknowledges financial support by the Swiss National Science Foundation, Ambizione Grant No. PZ00P2 161388.

[1] D. Shechtman, I. Blech, D. Gratias, and J. W. Cahn, Phys. Rev. Lett. **53**, 1951 (1984).
[2] D. Levine and P. J. Steinhardt, Phys. Rev. Lett. **53**, 2477 (1984).
[3] J. Y. Park, Science **309**, 1354 (2005).
[4] J. Y. Park, D. F. Ogletree, M. Salmeron, C. J. Jenks, P. A. Thiel, J. Brenner, and J. M. Dubois, J. Mater. Res. **23**, 1488 (2008).
[5] D. A. Rabson, Prog. Surf. Sci. **87**, 253 (2012).
[6] A. E. Filippov, A. Vanossi, and M. Urbakh, Phys. Rev. Lett. **104**, 074302 (2010).
[7] K. McLaughlin, D. Rabson, and P. Thiel, Phys. Rev. Lett. **107**, 209401 (2011).
[8] M. Hirano, K. Shinjo, R. Kaneko, and Y. Murata, Phys. Rev. Lett. **67**, 2642 (1991).
[9] M. Hirano and K. Shinjo, Wear **168**, 121 (1993).
[10] M. Dienwiebel, G. S. Verhoeven, N. Pradeep, J. W. M. Frenken, J. A. Heimberg, and H. W. Zandbergen, Phys. Rev. Lett. **92**, 126101 (2004).
[11] M. H. Müser, L. Wenning, and M. O. Robbins, Phys. Rev. Lett. **86**, 1295 (2001).
[12] A. S. de Wijn, Phys. Rev. B **86**, 085429 (2012).
[13] E. Koren, E. Lortscher, C. Rawlings, A. W. Knoll, and U. Duerig, Science **348**, 679 (2015).
[14] D. Dietzel, C. Ritter, T. Mönninghoff, H. Fuchs, A. Schirmeisen, and U. D. Schwarz, Phys. Rev. Lett. **101**, 125505 (2008).
[15] D. Dietzel, T. Mönninghoff, C. Herding, M. Feldmann, H. Fuchs, B. Stegemann, C. Ritter, U. D. Schwarz, and A. Schirmeisen, Phys. Rev. B **82**, 035401 (2010).
[16] D. Dietzel, M. Feldmann, U. Schwarz, H. Fuchs, and A. Schirmeisen, Phys. Rev. Lett. **111**, 235502 (2013).
[17] N. Varini, A. Vanossi, R. Guerra, D. Mandelli, R. Capozza, and E. Tosatti, Nanoscale **7**, 2093 (2015).
[18] A. N. Kolmogorov and V. H. Crespi, Phys. Rev. Lett. **85**, 4727 (2000).
[19] P. Stampfli, Helv. Phys. Acta **59**, 1260 (1986).
[20] N. Niizeki and H. Mitani, J. Phys. A: Math. Gen. **20**, L405 (1987).
[21] A. Kolmogorov and V. Crespi, Phys. Rev. B **71**, 235415 (2005).
[22] E. Koren and U. Duerig (unpublished).